

New *COL6A6* variant detected by whole-exome sequencing is linked to break points in intron 4 and 3'-UTR, deleting exon 5 of *RHO*, and causing adRP

Miguel de Sousa Dias,¹ Imma Hernan,¹ Barbara Delás,² Beatriz Pascual,¹ Emma Borràs,¹ Maria José Gamundi,¹ Begoña Mañé,¹ Patricia Fernández-San José,^{3,4} Carmen Ayuso,^{3,4} Miguel Carballo¹

¹Molecular Genetics Unit, Hospital of Terrassa, Barcelona, Spain; ²Ophthalmology Service, Hospital of Terrassa Barcelona, Spain; ³Department of Genetics, IIS-Jimenez Diaz Foundation (IIS-FJD), Madrid, Spain; ⁴Centre for Biomedical Network Research on Rare Diseases (CIBERER), ISCIII, Madrid, Spain

Purpose: This study aimed to test a newly devised cost-effective multiplex PCR assay for the molecular diagnosis of autosomal dominant retinitis pigmentosa (adRP), as well as the use of whole-exome sequencing (WES) to detect disease-causing mutations in adRP.

Methods: Genomic DNA was extracted from peripheral blood lymphocytes of index patients with adRP and their affected and unaffected family members. We used a newly devised multiplex PCR assay capable of amplifying the genetic loci of *RHO*, *PRPH2*, *RPI*, *PRPF3*, *PRPF8*, *PRPF31*, *IMPDI*, *NRL*, *CRX*, *KLHL7*, and *NR2E3* to molecularly diagnose 18 index patients with adRP. We also performed WES in affected and unaffected members of four families with adRP in whom a disease-causing mutation was previously not found.

Results: We identified five previously reported mutations (p.Arg677X in the *RPI* gene, p.Asp133Val and p.Arg195Leu in the *PRPH2* gene, and p.Pro171Leu and p.Pro215Leu in the *RHO* gene) and one novel mutation (p.Val345Gly in the *RHO* gene) representing 33% detection of causative mutations in our adRP cohort. Comparative WES analysis showed a new variant (p.Gly103Arg in the *COL6A6* gene) that segregated with the disease in one family with adRP. As this variant was linked with the *RHO* locus, we sequenced the complete *RHO* gene, which revealed a deletion in intron 4 that encompassed all of exon 5 and 28 bp of the 3'-untranslated region (UTR).

Conclusions: The novel multiplex PCR assay with next-generation sequencing (NGS) proved effective for detecting most of the adRP-causing mutations. A WES approach led to identification of a deletion in *RHO* through detection of a new linked variant in *COL6A6*. No pathogenic variants were identified in the remaining three families. Moreover, NGS and WES were inefficient for detecting the complete deletion of exon 5 in the *RHO* gene in one family with adRP. Carriers of this deletion showed variable clinical status, and two of these carriers had not previously been diagnosed with RP.

Retinitis pigmentosa (RP) is the most common form of inherited retinopathy [1-3], affecting more than 1.5 million people worldwide. RP displays all three modes of Mendelian inheritance—autosomal dominant (adRP), autosomal recessive (arRP), and X-linked (XLRP)—as well as digenic [4] and mitochondrial inheritance modes [5,6]. In particular, adRP has been associated with mutations in nearly 20 genes [6-8]. Over the last two decades, candidate genes associated with adRP in individual patients have been screened for mutations in different populations, using a variety of methods, including single-strand conformational polymorphism (SSCP), denaturing gradient gel electrophoresis (DGGE), and denaturing high-performance liquid chromatography (DHPLC) followed by direct genomic sequencing. Our group previously employed these methods to achieve molecular diagnosis of 23.5% (52 of 221) of families with adRP in a Spanish

population. More recently, mutation arrays have been used for surveys, accounting for identification of disease-causing mutations in 15.1% of patients with adRP [9].

There is growing interest in genetic diagnostics within current clinical practice, and next-generation DNA sequencing (NGS) technology is becoming increasingly necessary to characterize mutations that cause monogenic disease [10-12]. Several studies have reported massively parallel sequencing of RP candidate genes [13-18]. Clinical NGS molecular testing surveys of patients with RP have revealed that most adRP-causing mutations are detected in fewer than a dozen candidate genes [7,8].

We recently developed a cost-effective method of testing for mutations in 12 common adRP-associated genes that account for more than 95% of known mutations [19]. To improve our adRP molecular testing approach for routine use, we devised a new simple and robust multiplex PCR assay capable of amplifying the genetic loci of *RHO* (GeneID: 6010; OMIM 180380), *PRPH2* (GeneID: 5961; OMIM 179605),

Correspondence to: Miguel Carballo, Molecular Genetics Unit, Hospital of Terrassa, Barcelona, Spain; Phone: +34-93-7310007 (ext. 2161); FAX: +34-93-7319045; email: mcarballo@cst.cat

RPI (GeneID: 6101; OMIM [603937](#)), *PRPF3* (GeneID: 9129; OMIM [607301](#)), *PRPF8* (GeneID: 10594; OMIM [607300](#)), *PRPF31* (GeneID: 26121; OMIM [606419](#)), *IMPDH1* (GeneID: 3614; OMIM [146690](#)), *NRL* (GeneID: 4901; OMIM [162080](#)), *CRX* (GeneID: 1406; OMIM [602225](#)), *KLHL7* (GeneID: 55975; OMIM [611119](#)) and *NR2E3* (GeneID: 10002; OMIM [604485](#))—where most adRP-causing mutations have been reported. The decreasing costs of NGS technology allow the extension of this analysis to whole-exome sequencing (WES) of the index patients. However, the large number of genetic variants identified, even after filtering, makes it complicated and time-consuming to assess which variants are disease-causing. To improve this process, we developed a trio analysis in which we compared the common genetic variants found by WES in two patients with the variants identified in one unaffected member of a family with adRP.

In the present study, we tested this trio approach in four families with adRP who had been previously excluded for adRP-causing mutations by multiplex PCR and NGS. In one family with adRP, WES revealed a new genetic variant in the RP-unrelated gene *COL6A6* (GeneID: 131873), which segregates in a three-generation family with adRP with a variable clinical phenotype. However, this *COL6A6* genetic variant was considered to be linked to the deletion in *RHO* rather than causative of adRP. The present article also discusses the advantages and limitations of mutation detection using NGS and a comparative WES approach.

METHODS

Patients and DNA samples: The study was conducted in patients with retinitis pigmentosa who had been admitted to the Terrassa Hospital or sent from other Spanish hospitals. All patients underwent a full ophthalmic and electrophysiological [20] examination that included best-corrected visual acuity measurement with Snellen optotypes, intraocular pressure measurement, biomicroscopic slit-lamp examination and fundus examination, fundus photography, visual field testing with a Humphrey system 745I (Carl Zeiss, Barcelona, Spain), and full-field electroretinography. Macular anatomy was examined with ocular coherence tomography (Cirrus HD-OCT; Carl Zeiss). All patients gave informed consent before participation. This study adhered to the ARVO statement on human subjects, conducted in accordance with the Declaration of Helsinki and approved by the internal clinical research ethics committee (CEIC) of Terrassa Hospital, Spain.

A family with adRP was defined as a family with at least two affected members in successive generations, with or without male-to-male transmission. In families without male-to-male disease transmission, family members

were considered to have adRP if men and women showed similar clinical phenotypes or if an XLRP-linked association was previously excluded by linkage analysis of known XLRP loci. However, the possibility of XLRP linkage with complete penetrance in women in these families should not be discarded [8]. We obtained DNA from 18 adRP index cases. In 12 cases, DNA was isolated from peripheral blood lymphocytes via an automatic process using the MagNA Pure Compact Instrument (Roche, Barcelona, Spain) following the manufacturer's protocol. The other six DNA samples were obtained from the index cases of families with adRP who had been referred from centers in the [EsRetNet](#) network.

Oligonucleotide design and multiplex PCR amplification from gDNA: From GenBank, we obtained the genomic reference sequences for 11 adRP-associated genes: *CRX*, *IMPDH1*, *KLHL7*, *NRL*, *NR2E3*, *PRPF3*, *PRPF8*, *PRPF31*, *PRPH2* (*RDS*), *RHO*, and *RPI*. The oligonucleotide primers for multiplex PCR (Appendix 1) were designed using the Oligo 7.41 program (Molecular Biology Insights Colorado Springs, CO), with the aim of amplifying most of the coding exons and flanking splice junctions from each gene. The thermodynamic-based program [MFEprimer-2.0](#) was also used to check PCR primer specificity and compatibility [21,22]. To obtain each library, we used 44 pairs of primers divided into six-plex. Each forward and reverse primer included an M13 tag at the 5'-end for posteriori sequencer adaptor insertion (Appendix 1). Multiplex PCR reactions were performed in a 25- μ l reaction mix containing 20 ng gDNA as the template, using the Qiagen Multiplex PCR Kit (Qiagen, Barcelona, Spain) supplemented with a 0.5X final concentration of Q-Solution (Qiagen) and following the manufacturer's recommendations. Appendix 1 presents the specific plex conditions and primers used.

Chimerical sample preparation: We first conducted a pilot experiment to evaluate the appropriateness of the multiplex PCR method. This experiment comprised a parallel sequencing run of five chimerical samples prepared using DNA samples from several patients previously molecularly diagnosed with adRP. Each chimerical sample contained three point mutations distributed within its six-plex (Table 1), which helped evaluate the efficacy of this approach for successfully detecting genetic variations.

Library construction and sample-specific DNA barcode for parallel NGS: For each six-plex obtained per sample via the multiplex PCR assay, the DNA concentration was measured using an Epoch™ Microplate Spectrophotometer combined with the Take3™ Multi-Volume Plate (Izasa, Barcelona, Spain), following the manufacturer's instructions. The samples were then pooled at equal concentrations. To

simultaneously test several samples in a single sequencing run, each sample library was constructed using a specific adaptor. Each adaptor included a unique sequence of ten nucleotides (called the molecular identifier, MID) to distinguish each sample after NGS. The MID adaptors were inserted into the DNA fragments using a limited-cycle PCR (20 cycles at 95 °C for 30 s, 50 °C for 30 s 72 °C for 1 min), with a short M13-sequence tag included at the 5'-end of the specific primers. From the 454 Standard MID set (Roche), the present study used MIDs 1 to 5 (corresponding to chimerical samples 1 to 5; Table 1), and MIDs 1 to 18 (corresponding to the 18 analyzed index patients with adRP), which were compatible with the amplicon library protocol. The DNA libraries from each sample were then pooled so they could be clonally amplified through emulsion PCR and sequenced using the GS 454 Junior platform (Roche).

Clonal amplification of DNA libraries and NGS: Next, the DNA libraries generated from the multiplex system were clonally amplified. An emulsion PCR (emPCR) technique was performed following the instructions of the emPCR Amplification Method Manual-Lib-A (Roche). Once the DNA libraries possessed the sequencing adaptors (or MID adaptors) and had gone through the clonal amplification process, they were loaded into a PicoTiter sequencing plate (PTP). The sequencing run was prepared as described in the Sequencing Method Manual (GS Junior Titanium Series, Roche). DNA library sequencing was performed for 200 nucleotide cycles (approximately 500 bases) using a GS 454 Junior instrument (Roche) following the manufacturer's protocols.

Data analysis and variant annotation: The data from a sequencing run were processed using the GS Run Processor application to convert raw images into signal intensity values. The data processing steps were configured as part of the sequencing run using the Instrument Procedure Wizard, as described in the GS Sequencer application manual (Roche). Appendix 2 presents the data processing pipeline, specifying the options required to perform data processing with respect to what should be processed (the NGS libraries).

The processed and quality-filtered reads were then analyzed with the GS Amplicon Variant Analyzer (AVA) for the multiplex PCR assay analysis. The amplicons (excluding adaptors and MIDs) were used as the reference to align amplicon reads, and template-specific portions of the fusion primers were regarded as the forward and reverse primers. The known mutations in the selected samples were defined as substitutions relative to the reference sequence. Correspondence between the samples and MID tags was specified, and since the same MID was present in both orientations, an "either" encoding multiplexer was used to demultiplex the reads.

All sequence variants were named according to the Human Genome Variation Society's recommended guidelines, using the A of the ATG translation initiation codon as nucleotide +1. Each HCDiff was qualified as a single-nucleotide polymorphism (SNP) or a disease-causing mutation. Analysis for pathogenicity of genetic variants was performed using the SIFT, PolyPhen2, and MutationTaster algorithms.

TABLE 1. PREVIOUSLY IDENTIFIED GENETIC VARIANTS THAT WERE PRESENT IN THE 5 CHIMERICAL SAMPLES FROM SPANISH FAMILIES WITH adRP.

Chimerical sample	Gene	Variant	Protein change
1	<i>RHO</i>	c.119C>T	p.Leu40Pro
	<i>PRPF31</i>	c.735C>T	None (c.735C>T)
	<i>IMPDH1</i>	c.926G>C	p.Arg309Pro
2	<i>RHO</i>	c.644C>T	p.Pro215Leu
	<i>IMPDH1</i>	c.962C>T	p.Ala321Val
	<i>CRX</i>	c.425A>G	p.Try141Cys
3	<i>RHO</i>	c.1040C>T	p.Pro347Leu
	<i>PRPF8</i>	c.6968_6988del21bp	p.Val2325fsX2329
	<i>RPI</i>	c.2115delA	p.Lys705fsX712
4	<i>PRFP31</i>	c.669_770insA	p.Lys257fsX277
	<i>PRPF3</i>	c.1466C>A	p.Ala489Asp
	<i>RPI</i>	c.2038C>T	p.Arg677X
5	<i>RHO</i>	c.217_219delAAC	p.Asn73del
	<i>PRPF31</i>	c.328_330delATC	p.Ile109del
	<i>PRPH2</i>	c.641G>A	p.Cys214Tyr

Genetic variants that affected the splicing process were analyzed using NetGene2, NNSPLICE v0.9, Human Splicing Finder (HSF), and RESCUE-ESE.

WES analysis: Of the 18 families previously studied with multiplex PCR, four families (RPT65, SJD3, RPN83, and RPN89) were chosen for WES. From each family, we selected two affected members and one non-affected member to undergo WES comparative genetic variant analysis. Whole-exome capture was performed in accordance with the protocols for SureSelect All Human Enrichment Target Exon for 51 Mb (Agilent, Barcelona, Spain). The resulting library (500 ng) was hybridized to capture probes. Unhybridized material was washed away, and the captured fragments were amplified for ten PCR cycles, followed by purification using AMPure XP beads. The quality of the enriched libraries was evaluated using the 2100 Bioanalyzer and a High-Sensitivity DNA-kit (Agilent). The adaptor-ligated fragments were quantified with qPCR using the KAPA SYBR FAST library quantification kit for the Illumina Genome Analyzer (KAPA Biosystems, Woburn, MA). A 1-pM solution of the sequencing library was subjected to cluster generation for the HiSeq2000 following the manufacturer's instructions. Whole-exome sequencing was executed by Sistemas Genómicos (Valencia, Spain). The libraries were subjected to a clonal amplification process (cluster generation). The reactions for obtaining sequences of 100 nt × 2 (paired-end) were subsequently performed in the HiSeq2000 (Illumina, San Diego, CA) following the manufacturer's instructions.

Capillary Sanger sequencing and MLPA: Amplified products of mutation-positive or ambiguous samples were recovered from the plate, and column-purified using the High Pure PCR Product Purification Kit (Roche). These samples were then submitted to StabVida (Oeiras, Portugal) for direct sequencing on a 3730XL ABI DNA sequencer (Applied Biosystems, Foster City, CA) using the Big Dye terminator V1.1 DNA sequencing kit and the following PCR primers. The results were analyzed using FinchTV V1.4.0 software (Geospiza, Seattle, WA).

Multiplex ligation-dependent probe amplification (MLPA) reactions were performed using the SALSA® MLPA® P235 Retinitis probemix kit (MRC-Holland, Amsterdam, the Netherlands), which is designed to detect deletions/duplications of one or more sequences from *RHO* 3q21.3, *RPI* 8q11.2, *IMPDH1* 7q32, and *PRPF31* 19q13.4. Analyses were performed using Peak Scanner v1.0 (Applied Biosystems, Carlsbad, CA) and Coffalyser.Net software (MRC-Holland, Amsterdam, the Netherlands). Heterozygous deletions of recognition sequences were expected to produce a 35–50% reduced relative peak area for the amplification

product of that probe. For family RPT65, a heterozygous *RHO* deletion was detected using 1.5% agarose gel electrophoresis of the PCR fragments obtained using a forward primer (5'-TCA CGG CTC TGA GGG TCC A-3') that targets exon 4 and a reverse primer (5'-TGC CTC CTC CAC CTC TAG C-3') targeting the 3'-untranslated region (UTR) of *RHO* (NCBI Ref Seq NG_009115.1).

Retinal COL6A6 gene expression and genetic variant screening in families with adRP and the control population: To investigate retinal *COL6A6* expression, we performed PCR amplification of partial exons 2 and 3 from retinal PCR Ready First Strand cDNA (Amsbio, Barcelona Spain). Standard gel electrophoresis was used to detect the PCR fragment that was positive in cDNA and absent from gDNA. The novel genetic variant c.307G>A that causes a p.Gly103Arg change in *COL6A6* was investigated in 120 index patients with molecular undiagnosed adRP and 200 controls using real-time PCR with fluorescence resonance energy transfer (FRET) probes. The following primers and probes were used: forward, 5'-CCT GGC CCA GTA CAG TGA TAA A-3'; reverse 5'-GGG GAA ACT GTT TCT TGT CTC TC-3'; mut sensor probe, 5'-TGG ATT CAT TGG CAG GTC CC-FL-3'; and anchor probe, LC640-GCA GAT AGG AAA GGC TCT TCA GGA GGC T-p (synthesized by Tib Molbiol, Berlin, Germany).

RESULTS

Parallel mutation detection assay in adRP-associated genes by multiplex PCR and NGS: We constructed NGS libraries that contained more than 40 amplicons obtained by multiplex PCR of six-plex. These libraries were used to establish a mutation detection assay covering a gene panel of 11 candidate genes commonly associated with adRP. To evaluate the appropriateness of the multiplex PCR method, we first performed a pilot experiment consisting of a parallel sequencing run of chimerical samples 1 to 5. Variants detected in the chimerical samples using the GS Junior platform were then compared with those characterized by Sanger sequencing (Table 1). The sequenced parallel chimerical library generated 77,514 high-quality reads (28.3% of the total raw reads) in the GS Junior platform, of which 77,311 reads (99.71%) were successfully aligned with the references (Appendix 3). Among nearly 54.8% (42,511 raw reads) of the total high-quality reads, the average read length was 327 base pairs.

The resulting data generated from the parallel run were analyzed using the GS Amplicon Variant Analyzer (AVA) software version 2.5p1. Appendix 4 presents the average reads per amplicon obtained for each gene. High numbers of reads were obtained from all amplicons for all genes—except the

RPI gene, for which the number of reads ranged from 3 to 27. This could indicate some inhibition of the primers for exon 4 of the *RPI* gene by other primers in the Plex-E mix (Appendix 1). Although the established cut-off for molecular diagnosis is $>20\times$ reads (with 20–70% variation) in 454 pyrosequencing next generation sequencing (NGS) platforms, fewer than ten reads could also be evaluated with the 95% confidence level [23,24].

The adRP-associated point mutations found with the Sanger method were detected in the five chimerical samples (Table 2). These mutations were detected with a mean variation of 48.1% (range, 33.9% to 60.0%) with a resulting confidence level of 99.9% [24]. All point mutations were successfully detected with a read count of $>30\times$, with the exception of the *RPI* gene-related point mutations. For these mutations, only 15 reads were counted from chimerical sample 3 and 13 reads from chimerical sample 4. However, the primary mutations c.2115delA and c.2038C>T were still effectively detected, showing total variations of 40.0% and 53.9% in chimerical samples 3 and 4, respectively. These values showed a confidence level close to 99.9%, as is required for molecular diagnosis [23,24].

Molecular diagnosis of patients with adRP by multiplex PCR and NGS: To investigate the clinical use of our previously described multiplex PCR approach, we used this approach to analyze 18 patients with an uncharacterized adRP-causing mutation. This analysis was performed through three distinct NGS runs, each containing a library constructed using DNA from six patients. Appendix 5 shows the average data from

NGS runs. NGS data analysis revealed six different mutations (Table 3), which were confirmed by capillary Sanger sequencing. We detected the novel genetic variant c.1034T>G (Val345Gly) in *RHO*, which segregated in family RPT100 (Figure 1) and was also tested by capillary Sanger sequencing. In our survey using the multiplex PCR and NGS approach, successful molecular diagnosis was achieved in six (33.3%) of the 18 index patients with adRP.

Assay for molecular diagnosis of adRP families by WES: Of the families with adRP for which a disease-causing mutation was not detected by the multiplex PCR approach, four families (SJD3, RPT65, RPN83, and RPN89) were chosen to undergo comparative WES analysis. The aim was to investigate the usefulness of this technique in molecular diagnosis of adRP and/or to find new adRP-associated genes. We used a trio strategy to find variants that were shared by two related patients with RP but absent in an unaffected family member. The two affected relatives analyzed with WES were selected to be as distantly related as possible to avoid the maximum common genetic variants. WES analysis of the four families with adRP revealed an average of 80 new genetic variants (not annotated in a database) and 110 annotated genetic variants, with a frequency of <0.01 . One candidate genetic variant—c.307G>A (p.Gly103Arg) in the *COL6A6* gene, which was found only in family RPT65—was identified as a strong candidate based on cosegregation in a four-generation family with adRP, absence in controls, and in silico analysis (see below). No obvious pathogenic genetic

TABLE 2. MUTATIONS DETECTED FOR EACH OF THE CHIMERIC SAMPLES USING MULTIPLEX PCR AND NEXT-GENERATION SEQUENCING.

Chimerical/MID	Gene	Variant	% Variant	Reads per amplicon
1	<i>RHO</i>	c.119C>T	60.0	30
	<i>PRPF31</i>	c.735C>T	50.7	301
	<i>IMPDH1</i>	c.926G>C	42.3	167
2	<i>RHO</i>	c.644C>T	33.9	149
	<i>IMPDH1</i>	c.962C>T	56.4	126
	<i>CRX</i>	c.425A>G	49.6	140
3	<i>RHO</i>	c.1040C>T	51.2	84
	<i>PRPF8</i>	c.6968_6988del21bp	48.7	394
	<i>RPI</i>	c.2115delA	40.0	15
4	<i>PRPF31</i>	c.669_770insA	35.0	314
	<i>PRPF3</i>	c.1466C>A	45.9	715
	<i>RPI</i>	c.2038C>T	53.9	13
5	<i>RHO</i>	c.217_219delAAC	58.1	74
	<i>PRPF31</i>	c.328_330delATC	45.4	326
	<i>PRPH2</i>	c.641G>A	50.5	309

TABLE 3. VARIANTS CAUSING ADRP THAT WERE FOUND IN 18 PATIENTS STUDIED USING THE MULTIPLEX-PCR APPROACH.

Sample	Gene	Variant	% Variant	Reads per amplicon	Protein change	HGMD*
RPT65**	RHO	(g.9281_10108del)	–	–	Truncated	New
RPT100	RHO	c.1034T>G	44.6	65	p.Val1345Gly	New
RPN235	RPI	c.2029C>T	62.5	19	p.Arg677X	CM991103
RP208	PRPH2	c.518A>T	64.3	68	p.Asp173Val	CM941209
RP227	RHO	c.512C>T	63.0	54	p.Pro171Leu	CM910335
Tek14	PRPH2	c.584G>T	42.9	163	p.Arg195Leu	CM032999
RPN240	RHO	c.644C>T	53.9	127	p.Pro215Leu	CM003954

*Human Gene Mutation Database **Genetic variant not detected by multiplex PCR and NGS

variants were identified in the remaining three families, and further analysis of these families is ongoing.

New genetic variant in COL6A6 detected by WES cosegregates in one family with adRP: Appendix 6 shows the candidate genetic variants found by WES in family RPT65, which were validated using direct capillary Sanger sequencing and segregated in the family. The new genetic variant c.1034T>G (p.Gly103Arg) in COL6A6 was the only variant in the family that cosegregated with the phenotype (Figure 2). The presence of the genetic variant c.1034T>G in the RPT65 family was validated by FRET assay (Appendix 7). We also used FRET to screen for this genetic variant in 120 index patients with adRP (in which the adRP-causing mutation is still unknown) and in 200 controls, none of whom exhibited the p.Gly103Arg genetic variant in COL6A6. PCR amplification of a fragment containing the juxtaposing sequences of exons 2 and 3 from a retinal cDNA sample revealed retinal expression of COL6A6.

Exon 5 deletion in RHO linked to the new genetic variant of COL6A6: The COL6A6 gene was located in chromosome 3 only 1 Mbp away from RHO loci, a gene where most

adRP-causing mutations are identified. Thus, we performed MPLA analysis to determine whether there was an abnormal copy number of genomic DNA sequences at the RHO locus. The results showed a nearly 30% reduction (not shown) in one probe that targets exon 5 of RHO, suggesting a deletion in this locus. Direct genomic sequencing of the complete RHO gene revealed a deletion beginning in intron 4 (g.9281_10108del) encompassing all of exon 5 and 28 bp of the 3'-UTR. PCR amplification was also performed to detect this RHO deletion and to segregate it within family RPT65 (Figure 2B). This deletion (g.9281_10108del) was present in all patients and carriers of the new COL6A6 genetic variant, showing the linkage between both variants. Moreover, unaffected members of the family did not carry either of these genetic variants, showing no recombinants for the variants within the RTP65 family.

Ophthalmic examination: Table 4 and Table 5 show the clinical features of the families RPT100 (Figure 1) and RT65 (Figure 2), who carried novel rhodopsin mutations found in our survey. Initially, we knew only the II:1 branch of the

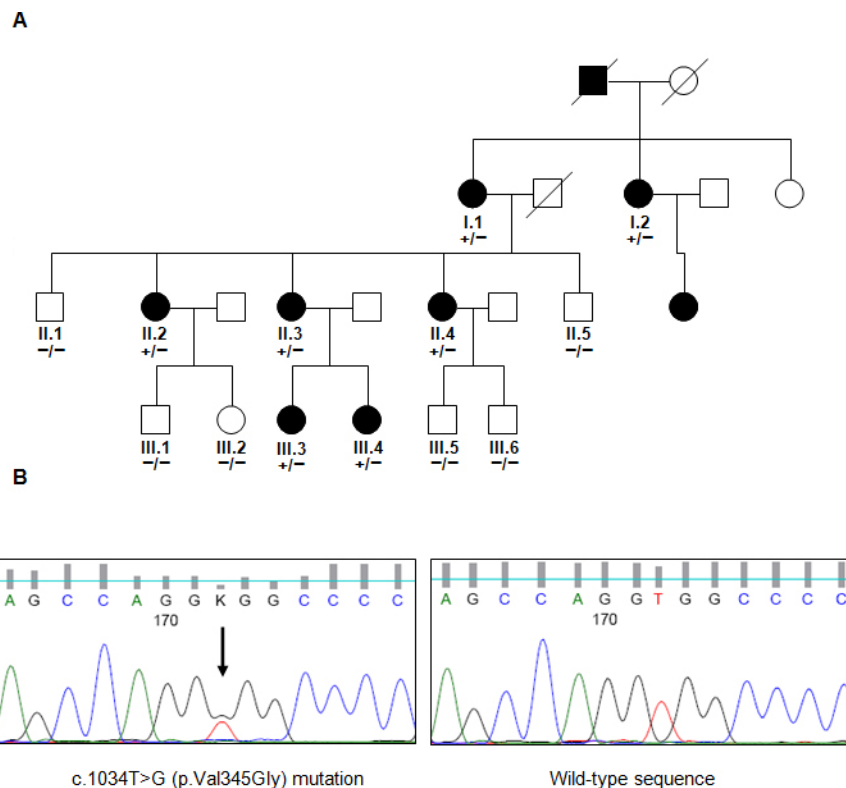


Figure 1. Pedigree and Sanger sequencing of family RPT100. **A:** Pedigree of the adRP family RPT100, which carries the mutation p.Val345Gly in RHO. Capillary Sanger sequencing showed either the presence of the mutation (+) or of the wild-type allele (-). Squares and circles represent men and women, respectively. The open symbols represent unaffected family members, while the completely filled symbols represent patients with retinitis pigmentosa (RP). **B:** Fluorogram representation of the Sanger sequencing of mutation c.1034T>G in the RHO gene.

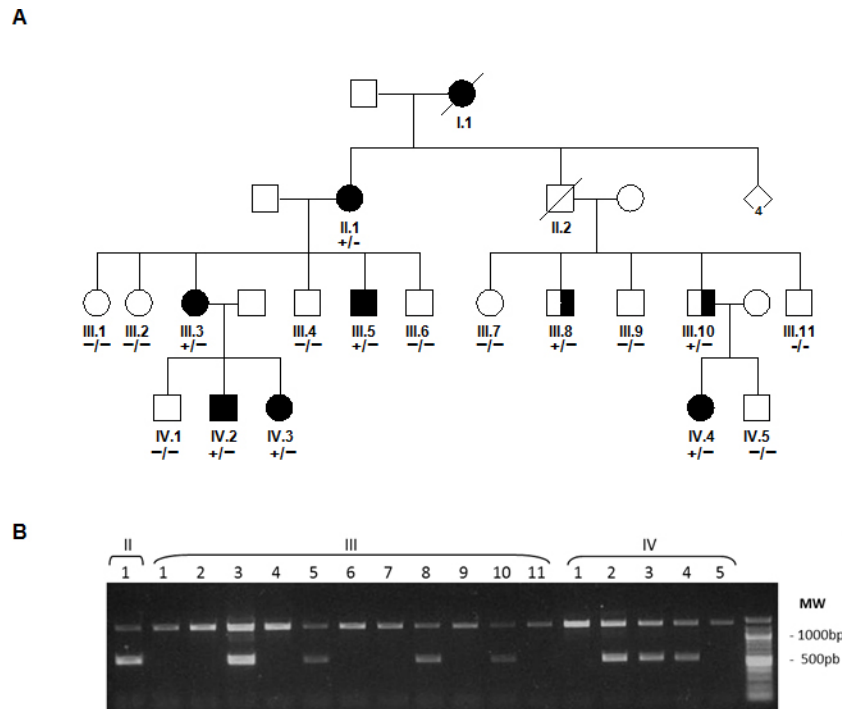


Figure 2. Pedigree and gel electrophoresis analysis of family RPT65. **A:** Pedigree of the adRP family RPT65, which carries the genetic variant c.307G> (p.Gly103Arg) causing the COL6A6/827-bp deletion (g.9281_10108del) in RHO. The genetic variant in COL6A6 was detected by capillary Sanger sequencing and fluorescence resonance energy transfer (FRET) assay, with (+) indicating the presence of genetic variants and (-) indicating wild-type alleles. Squares and circles represent men and women, respectively. The open symbols represent unaffected family members. Completely filled symbols represent patients with retinitis pigmentosa who underwent ophthalmic examination before genetic variant analysis was performed. Semifilled symbols represent carriers of the genetic variants who were not clinically diagnosed with RP before the molecular analysis. Ophthalmic examination of III:8 and III:10 showed a RP phenotype. **B:** Gel electrophoresis of the PCR products obtained by amplification of genomic DNA from the family members showing the deletion (g.9281_10108del) in RHO.

RPT65 family, who had been ophthalmologically examined and followed for years in our hospital (Table 5). They showed early onset of symptoms, including the appearance of night blindness during their early 20s. Fundus examination showed bone spicules, attenuated blood vessels, and optic disc pallor that worsened with age. Visual field testing revealed important visual field constriction in the patients' 20s, with normal function of the foveal photoreceptors allowing good central vision up until the end-stage of the disease (Figure

3 and Figure 4). Affected family members who were previously diagnosed with RP (descendants of II:1) experienced a slow rate of vision loss and had a more pericentral pattern of degeneration and pigment deposition.

Soon after discovering the p.Gly103Arg variant in COL6A6 among the descendants of II:1, we found in the central region of Spain a family branch of II:2 who had recently noticed the disease in their family. Member IV:4 was clinically diagnosed with RP after an ophthalmic

TABLE 4. CLINICAL FEATURES OF ADRP FAMILY RPT100 CARRYING THE p.Val345Gly MUTATION IN RHO.

Family member	Age (years)	Onset of NB	Current VFC	Current VA/BE	Current ERG	Funduscopy
II-2	57	25	<10° central	10/200	Not detectable	Typical RP
II-3	54	5	<10° central	10/200* 20/50**	Not detectable	Typical RP
II-4	50	14	<10° central	20/30* LP**	Not detectable	Typical RP
III-3	28	10	<10° central	20/30	Not detectable	Typical RP
III-4	23	12	<10° central	20/30	Not detectable	Typical RP

NB, night blindness; VFC, visual field constriction; VA, visual acuity; BE, both eyes; LP, light perception *right eye **left eye

TABLE 5. CLINICAL FEATURES OF adRP FAMILY RPT65 CARRYING THE G.9281 _ 10108DEL MUTATION IN RHO.

Family member	Age (years)	Onset of NB	Current VFC	Current VA/ BE	Current ERG	Funduscopy
III-3	61	14	<10° central	20/30	Not detectable	Typical RP
III-10	43	N/A	<10° central	20/25 25/25	N/A	Typical RP
IV-2	37	10	<10° central	20/20	Not detectable	Typical RP
IV-3	36	13	<10° central	20/20	Not detectable	Typical RP
IV-4	9	9	<10° central	20/20	Severe loss of amplitude in scotopic, maxima, and photopic responses	Typical RP

NB, night blindness; VFC, visual field constriction; VA, visual acuity; BE, both eyes, N/A not applicable

examination prompted by experiencing certain vision difficulties in semidarkness. Segregation analysis with FRET and capillary sequencing of the *COL6A6* genetic variant in the family branch descendent of II:2 (Figure 2) showed that the affected member IV:4 and the undiagnosed III:8 and III:10 were carriers. These undiagnosed carriers III:8 and III:10 were ophthalmologically examined after detection of the mutation. Their fundus examinations showed typical RP signs, although the patients stated that they were unaware of the disease. Some family members reported that they had

not noticed any visual impairment in the obligate carrier II:2, who died at the age of 83 years. Finally, we found that all carriers of the novel *COL6A6* genetic variant p.Gly103Arg in this family were also carriers of the 827-bp deletion (g.9281_10108del) in *RHO* (Figure 2).

DISCUSSION

In the present study, we analyzed 18 families with adRP to detect mutations in the genetic loci most commonly associated with adRP. We previously devised a robust and rapid

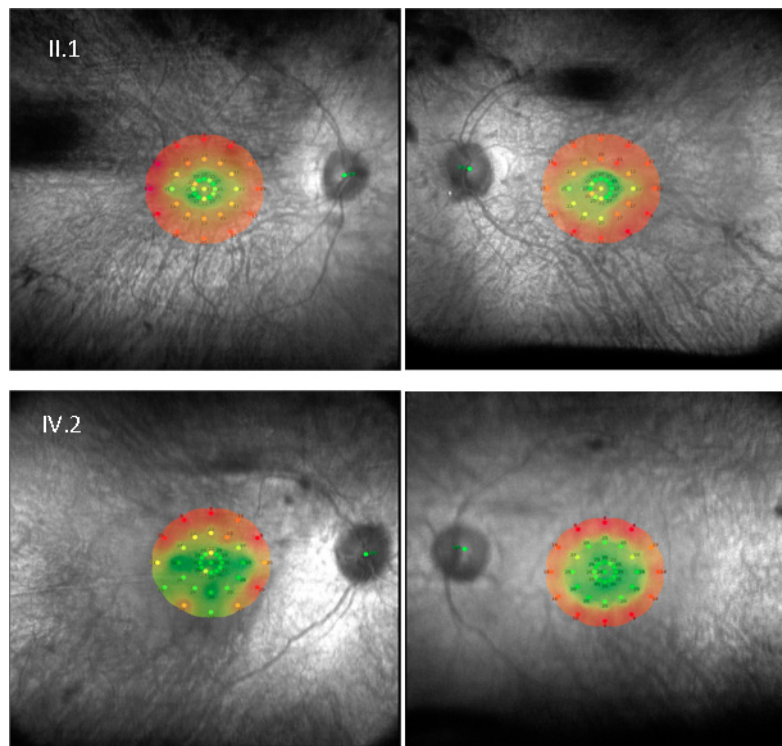


Figure 3. Lower macular sensitivity is shown with age. Microperimetric map image (MAIA, Topcon) of II:1 and son IV:2 (from family RPT65) who show normal sensitivity in the central macula (green area) and decreased sensitivity at the peripheral macula (red area). Thirty-six stimulus locations covering the central 10° field were tested.

method that uses multiplex PCR and an NGS benchtop platform, and that can be performed in any routine molecular genetics laboratory. This method is simple and cost-effective for the analysis of individual or few samples, which matches the current demand of laboratories in clinical hospitals. Our estimated cost for the analysis of six samples in a parallel run is approximately €200 using a GS Junior platform. Using this method revealed the disease-causing mutation in 33.3% of Spanish families with adRP, even when the mutation was new (p.Val345Gly in *RHO*). There are several possible explanations for the lack of detection of a disease-causing mutation in >60% of Spanish families who were analyzed for the most common adRP-associated genes, here and in previous studies [9,25]. Some of these families may actually have XLRP with female carriers who express the clinical phenotype of RP [8]. It is also possible that the mutation causing adRP is in an unknown gene or otherwise escapes the detection methods used. We reevaluated the families with adRP for mutation detection and selected those with male-to-male disease transmission as well as families that had been previously excluded for XLRP by linkage analysis.

In an attempt to find new adRP-associated mutations, three years earlier we had analyzed five index patients by

DNA target capture and NGS using a panel of 448 genes, including those known to be associated with RP [26]. However, the present cost of WES is nearly ten times lower than it was when the previous candidate gene panel was performed. The advancements and cost decreases in WES analysis led us to evaluate this methodology for possible routine molecular diagnostics of adRP. The large number of individual genetic variants necessitates analysis using at least trios of family individuals. Thus, the standard cost of €850 per sample should be at least tripled for WES analysis. Moreover, to minimize the common genetic variants, the analysis should include patients with the most minor possible relationship (e.g., different family generations). This limits the potential of WES as molecular diagnosis for use only in families with a large number of individuals available (both patients and unaffected family members). Additionally, characterization of a disease-causing mutation usually requires costly and time-consuming work for segregation of the identified candidate genetic variants (an average of 80). This limits the use of WES in routine molecular diagnosis and circumscribes its use in the detection of new genetic disease-causing variants.

We used WES to analyze genetic variants in the II:1 branch of family RPT65. Comparative analysis of the new

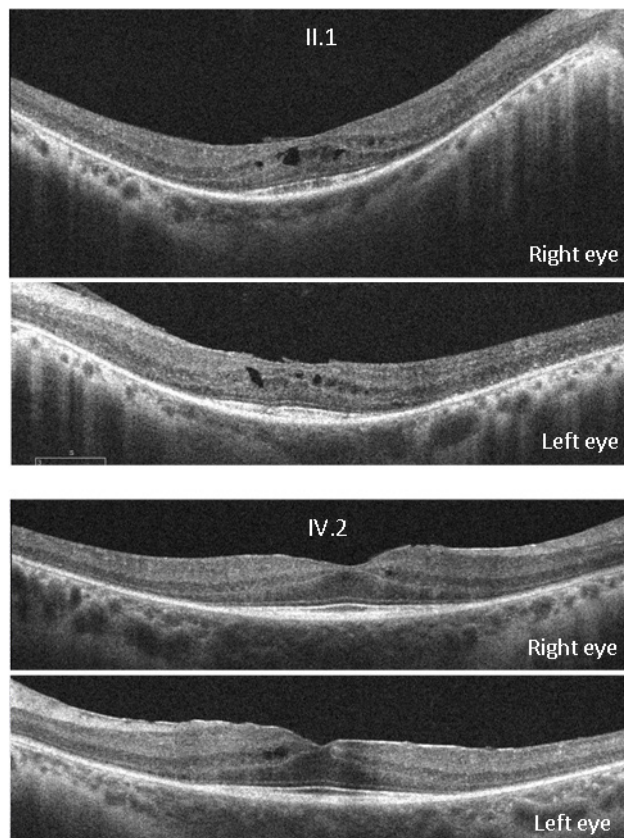


Figure 4. In the upper two panels, an OCT image of a 5-mm horizontal scan shows a distinct and continuous IS/OS line, correlating with the 20/20 visual acuity in the right eye of patient IV:2 from family RPT65. In the lower two panels, intraretinal cysts in the intermediate retina and abnormally structured IS/OS line correlate with the mother's (II:1) poorer visual acuity in the right eye (20/30).

genetic variants that were present in patients and absent in the unaffected family member revealed a list of 21 candidate variants—of which only c.307G>A (p.Gly103Arg) in the *COL6A6* gene cosegregated with the clinically diagnosed patients with RP. This variant was also present in the obligate III:10 carrier and in family member III:8 who was not previously diagnosed with RP. We positively characterized this new genetic variant as a possible cause of adRP, showing that it was absent in the 200 analyzed controls. We also demonstrated that the *COL6A6* gene was expressed in the retina. However, no functional analysis was performed because, presumably, the *COL6A6* protein [27] plays a structural role in the retina rather than a function that is measurable in vitro.

Based on these data and the standard criteria used for finding rare disease-causing variants using WES [28-30], the p.Gly103Arg variation in the *COL6A6* gene could be considered a strong candidate for the cause of adRP in the RPT65 family. Moreover, in silico analysis of this genetic variant by different approaches (including SIFT, PolyPhen, and MutationTaster) all predicted pathogenicity for the change p.Gly103Arg in the *COL6A6* protein. This result could be interpreted as the final point in a WES analysis that results in the identification of a novel disease-causing mutation in a new adRP-associated gene. When possible, the complete characterization of a novel gene associated with a genetic disease should involve a functional test. However, the positive data obtained by WES are sufficient that *COL6A6* could be considered a marker for disease-causing in this family.

The locus of *COL6A6* in chromosome 3 is nearly 1 Mbp from the rhodopsin gene, where most adRP-causing mutations have been found. In this family, *RHO* had been previously screened for mutation, but no *RHO* gene mutation was detected either with DGGE or with NGS analysis. As has been previously pointed out [29,31-33], the usefulness of these techniques may be limited in the case of a mutation that encompasses intronic regions or deletions that affect the amplification or target capture. Sanger sequencing of the complete *RHO* gene in the family revealed an 827-bp deletion (g.9281_10108del) in intron 4 that encompassed all of exon 5 and 28 bp of the 3'-UTR of *RHO*. In detection methods that rely on PCR amplification, such as DGGE and multiplex PCR, the reverse primer used was placed over only the deleted 3' region of *RHO*, and thus, only the wild-type allele was amplified. However, revision of the read coverage in our NGS assays of the *RHO*-deleted region showed that the results were insufficient to detect the deletion mutation.

If translated to the protein, the mutant allele g.9281_10108del may cause a pathogenic mechanism through a dominant-negative effect. If this mutant *RHO* is

not translated or is processed by a nonsense-mediated mRNA decay (NMD) mechanism, it could lead to a haploinsufficiency effect. Similar to this deletion of exon 5 of *RHO*, two Scottish families with adRP reportedly showed a G-to-A transition in the highly conserved AG dinucleotide in the 3'-acceptor splice site of exon 4 of *RHO* [34]. This mutation, revealed by illegitimate transcription analysis of circulating blood lymphocytes, shows an aberrant RNA product in which exon 4 is spliced with an adenine of the 3'-UTR of *RHO*, thus excluding exon 5 plus 143 bp of the 3'-UTR [35]. However, there is currently no evidence that this mutant is translated to a protein.

The RP-affected carriers of the mutation g.9281_10108del in *RHO* showed a phenotype that included early-onset night blindness and bone spicules, with slow disease progression. These patients with RP showed relatively well-conserved visual function compared with most other patients carrying an *RHO* mutation—for example, the p.Val345Gly carriers, in whom RP causes early visual impairment. However, mild or even recessive RP phenotypes caused by *RHO* mutations have been previously reported in carriers of some mutations that predict splicing alteration or a truncated protein [36-41]. Revision of the RP phenotype associated with mutations in *PRPF8* (a splicing pre-mRNA factor) leads to an early-onset severe alteration in the peripheral retina, but the patients generally retain good visual acuity until the fifth or sixth decade of life [42,43]. These RP phenotypes are comparable with the ones presently observed in patients with the *RHO* gene deletion of exon 5. It can be speculated that there is a convergent pathogenic mechanism caused by *RHO* haploinsufficiency, with a lack of rhodopsin due to an untranslated mutated protein and an insufficient *RHO* splicing rate caused by a mutation in *PRPF8*.

APPENDIX 1. MULTIPLEX-PCR CONDITIONS FOR NGS TARGET ENRICHMENT (PLEX A TO F).

To access the data, click or select the words “[Appendix 1.](#)”

APPENDIX 2. WORKFLOW OF THE DATA PROCESSING SCHEME IN THE GS JUNIOR SYSTEM FOR AMPLICON ANALYSIS. THE BLOCKS IDENTIFY THE VARIOUS DATA ACQUISITION, DATA PROCESSING, OR DATA ANALYSIS APPLICATIONS AND THEIR OUTPUTS.

To access the data, click or select the words “[Appendix 2.](#)”

APPENDIX 3. SEQUENCE READS OBTAINED BY NGS IN THE PARALLEL RUN OF THE CHIMERICAL SAMPLE.

To access the data, click or select the words “[Appendix 3.](#)”

APPENDIX 4. AVERAGE NUMBER OF READS PER AMPLICON FOR EACH GENE ANALYZED.

To access the data, click or select the words “[Appendix 4.](#)”

APPENDIX 5. AVERAGE NUMBER OF READS PER AMPLICON FOR EACH ANALYZED GENE AMONG THE 18 PATIENTS.

To access the data, click or select the words “[Appendix 5.](#)”

APPENDIX 6. VARIANTS SELECTED FOR SEGREGATION STUDIES.

To access the data, click or select the words “[Appendix 6.](#)”
Bold type line shows the only identified genetic variant that co-segregated with RP in the RPT65 family.

APPENDIX 7. FLUORESCENCE RESONANCE ENERGY TRANSFER (FRET) METHOD USED FOR SCREENING THE GENETIC VARIANT C.307G>A IN COL6A6 IN ADRP INDEX PATIENTS AND A CONTROL SPANISH POPULATION.

To access the data, click or select the words “[Appendix 7.](#)”
FRET fluorogram shows a sample that was wild-type (red peak) and one that was heterozygous (blue double peak) for the genetic variant.

ACKNOWLEDGMENTS

We thank San Francisco Edit and Ian Johnstone for help with editing this manuscript. This work was partially supported by grants from the Fondo de Investigaciones Sanitarias (PS0901271, PI0990754, PI1200246).

REFERENCES

1. Kennan A, Aherne A, Humphries P. Light in retinitis pigmentosa. *Trends in genetics TIG* 2005; 21:103-10. [PMID: 15661356].
2. Hartong DT, Berson EL, Dryja TP. Retinitis pigmentosa. *Lancet* 2006; 368:1795-809. [PMID: 17113430].
3. Goodwin P. Hereditary retinal disease. *Curr Opin Ophthalmol* 2008; 19:255-62. [PMID: 18408503].
4. Kajiwara K, Berson EL, Dryja TP. Digenic retinitis pigmentosa due to mutations at the unlinked peripherin/RDS and ROM1 loci. *Science* 1994; 264:1604-8. [PMID: 8202715].
5. Rivolta C, Sharon D, DeAngelis MM, Dryja TP. Retinitis pigmentosa and allied diseases: numerous diseases, genes, and inheritance patterns. *Hum Mol Genet* 2002; 11:1219-27. [PMID: 12015282].
6. Daiger SP, Bowne SJ, Sullivan LS. Perspective on genes and mutations causing retinitis pigmentosa. *Arch Ophthalmol* 2007; 125:151-8. [PMID: 17296890].
7. Sullivan LS, Bowne SJ, Birch DG, Hughbanks-Wheaton D, Heckenlively JR, Lewis RA, Garcia CA, Ruiz RS, Blanton SH, Northrup H, Gire AI, Seaman R, Duzkale H, Spellicy CJ, Zhu J, Shankar SP, Daiger SP. Prevalence of disease-causing mutations in families with autosomal dominant retinitis pigmentosa: a screen of known genes in 200 families. *Invest Ophthalmol Vis Sci* 2006; 47:3052-64. [PMID: 16799052].
8. Bowne SJ, Sullivan LS, Koboldt DC, Ding L, Fulton R, Abbott RM, Sodergren EJ, Birch DG, Wheaton DH, Heckenlively JR, Liu Q, Pierce EA, Weinstock GM, Daiger SP. Identification of disease-causing mutations in autosomal dominant retinitis pigmentosa (adRP) using next-generation DNA sequencing. *Invest Ophthalmol Vis Sci* 2011; 52:494-503. [PMID: 20861475].
9. Blanco-Kelly F, García-Hoyos M, Cortón M, Avila-Fernández A, Riveiro-Alvarez R, Gimenez A, Hernan I, Carballo M, Ayuso C. Genotyping microarray: mutation screening in Spanish families with autosomal dominant retinitis pigmentosa. *Mol Vis* 2012; 18:1478-83. [PMID: 22736939].
10. ten Bosch JR, Grody WW. Keeping up with the next generation: massively parallel sequencing in clinical diagnostics. *The Journal of molecular diagnostics JMD* 2008; 10:484-92. [PMID: 18832462].
11. Voelkerding KV, Dames SA, Durtschi JD. Next-generation sequencing: from basic research to diagnostics. *Clin Chem* 2009; 55:641-58. [PMID: 19246620].
12. Kuhlenbäumer G, Hullmann J, Appenzeller S. Novel genomic techniques open new avenues in the analysis of monogenic disorders. *Hum Mutat* 2011; 32:144-51. [PMID: 21280146].
13. Neveling K, Collin RW, Gilissen C, van Huet RA, Visser L, Kwint MP, Gijzen SJ, Zonneveld MN, Wieskamp N, de Ligt J, Siemiatkowska AM, Hoefsloot LH, Buckley MF, Kellner U, Branham KE, den Hollander AI, Hoischen A, Hoyng C, Klevering BJ, van den Born LI, Veltman JA, Cremers FP, Scheffer H. Next-generation genetic testing for retinitis pigmentosa. *Hum Mutat* 2012; 33:963-72. [PMID: 22334370].
14. Simpson DA, Clark GR, Alexander S, Silvestri G, Willoughby CE. Molecular diagnosis for heterogeneous genetic diseases with targeted high-throughput DNA sequencing applied to retinitis pigmentosa. *J Med Genet* 2011; 48:145-51. [PMID: 21147909].
15. O’Sullivan J, Mullaney BG, Bhaskar SS, Dickerson JE, Hall G, O’Grady A, Webster A, Ramsden SC, Black GC. A paradigm shift in the delivery of services for diagnosis of inherited retinal disease. *J Med Genet* 2012; 49:322-6. [PMID: 22581970].

16. Shanks ME, Downes SM, Copley RR, Lise S, Broxholme J, Hudspith KA, Kwasniewska A, Davies WI, Hankins MW, Packham ER, Clouston P, Seller A, Wilkie AO, Taylor JC, Ragoussis J, Nemeth AH. Next-generation sequencing (NGS) as a diagnostic tool for retinal degeneration reveals a much higher detection rate in early-onset disease. *European journal of human genetics* 2013; 21:274-80. [PMID: 22968130].
17. Glöckle N, Kohl S, Mohr J, Scheurenbrand T, Sprecher A, Weisschuh N, Bernd A, Rudolph G, Schubach M, Poloschek C, Zrenner E, Biskup S, Berger W, Wissinger B, Neidhardt J. Panel-based next generation sequencing as a reliable and efficient technique to detect mutations in unselected patients with retinal dystrophies. *European journal of human genetics* Eur J Hum Genet 2014; 22:99-104. [PMID: 23591405].
18. Fu Q, Wang F, Wang H, Xu F, Zaneveld JE, Ren H, Keser V, Lopez I, Tuan HF, Salvo JS, Wang X, Zhao L, Wang K, Li Y, Koenekoop RK, Chen R, Sui R. Next-generation sequencing-based molecular diagnosis of a Chinese patient cohort with autosomal recessive retinitis pigmentosa. *Invest Ophthalmol Vis Sci* 2013; 54:4158-66. [PMID: 23661369].
19. de Sousa Dias M, Hernan I, Pascual B, Borrás E, Mañe B, Gamundi MJ, Carballo M. Detection of novel mutations that cause autosomal dominant retinitis pigmentosa in candidate genes by long-range PCR amplification and next-generation sequencing. *Mol Vis* 2013; 19:654-64. [PMID: 23559859].
20. Standard for clinical electroretinography. International Standardization Committee. *Arch Ophthalmol* 1989; 107:816-9. [PMID: 2730397].
21. Qu W, Shen Z, Zhao D, Yang Y, Zhang C. MFEprimer: multiple factor evaluation of the specificity of PCR primers. *Bioinformatics* 2009; 25:276-8. [PMID: 19038987].
22. Qu W, Zhou Y, Zhang Y, Lu Y, Wang X, Zhao D, Yang Y, Zhang C. MFEprimer-2.0: a fast thermodynamics-based program for checking PCR primer specificity. *Nucleic Acids Res* 2012; 40:W205-8. [PMID: 22689644].
23. Brockman W, Alvarez P, Young S, Garber M, Giannoukos G, Lee WL, Russ C, Lander ES, Nusbaum C, Jaffe DB. Quality scores and SNP detection in sequencing-by-synthesis systems. *Genome Res* 2008; 18:763-70. [PMID: 18212088].
24. De Leeneer K, De Schrijver J, Clement L, Baetens M, Lefever S, De Keulenaer S, Van Criekinge W, Deforce D, Van Nieuwerburgh F, Bekaert S, Pattyn F, De Wilde B, Coucke P, Vandesompele J, Claes K, Hellemans J. Practical tools to implement massive parallel pyrosequencing of PCR products in next generation molecular diagnostics. *PLoS ONE* 2011; 6:e25531. [PMID: 21980484].
25. Millá E, Maseras M, Martínez-Gimeno M, Gamundi MJ, Assaf H, Esmerado C, Carballo M, Grupo Multicéntrico Español de Retinosis P. Genetic and molecular characterization of 148 patients with autosomal dominant retinitis pigmentosa (ADRP). *Arch Soc Esp Oftalmol* 2002; 77:481-4. [PMID: 12221539].
26. Borrás E, de Sousa Dias M, Hernan I, Pascual B, Mañe B, Gamundi MJ, Delás B, Carballo M. Detection of novel genetic variation in autosomal dominant retinitis pigmentosa. *Clin Genet* 2013; 84:441-52. [PMID: 23534816].
27. Fitzgerald J, Holden P, Hansen U. The expanded collagen VI family: new chains and new questions. *Connect Tissue Res* 2013; 54:345-50. [PMID: 23869615].
28. Bamshad MJ, Ng SB, Bigham AW, Tabor HK, Emond MJ, Nickerson DA, Shendure J. Exome sequencing as a tool for Mendelian disease gene discovery. *Nat Rev Genet* 2011; 12:745-55. [PMID: 21946919].
29. Eisenberger T, Neuhaus C, Khan AO, Decker C, Preising MN, Friedburg C, Bieg A, Gliem M, Charbel Issa P, Holz FG, Baig SM, Hellenbroich Y, Galvez A, Platzer K, Wollnik B, Laddach N, Ghaffari SR, Rafati M, Botzenhart E, Tinschert S, Borger D, Bohring A, Schreml J, Kortge-Jung S, Schell-Apacic C, Bakur K, Al-Aama JY, Neuhann T, Herkenrath P, Nurnberg G, Nurnberg P, Davis JS, Gal A, Bergmann C, Lorenz B, Bolz HJ. Increasing the yield in targeted next-generation sequencing by implicating CNV analysis, non-coding exons and the overall variant load: the example of retinal dystrophies. *PLoS ONE* 2013; 8:e78496. [PMID: 24265693].
30. Linderman MD, Brandt T, Edelmann L, Jabado O, Kasai Y, Kornreich R, Mahajan M, Shah H, Kasarskis A, Schadt EE. Analytical validation of whole exome and whole genome sequencing for clinical applications. *BMC Med Genomics* 2014; 7:20. [PMID: 24758382].
31. Fang H, Wu Y, Narzisi G, O'Rawe JA, Barron LT, Rosenbaum J, Ronemus M, Iossifov I, Schatz MC, Lyon GJ. Reducing INDEL calling errors in whole genome and exome sequencing data. *Genome Med.* 2014; 6:89. [PMID: 25426171].
32. Meynert AM, Ansari M, FitzPatrick DR, Taylor MS. Variant detection sensitivity and biases in whole genome and exome sequencing. *BMC Bioinformatics* 2014; 15:247. [PMID: 25038816].
33. Tan R, Wang Y, Kleinstein SE, Liu Y, Zhu X, Guo H, Jiang Q, Allen AS, Zhu M. An evaluation of copy number variation detection tools from whole-exome sequencing data. *Hum Mutat* 2014; 35:899-907. [PMID: 24599517].
34. Bell C, Converse CA, Hammer HM, Osborne A, Haites NE. Rhodopsin mutations in a Scottish retinitis pigmentosa population, including a novel splice site mutation in intron four. *Br J Ophthalmol* 1994; 78:933-8. [PMID: 7819178].
35. Whitehead JL, Bell C, Converse CA, Hammer HM, Haites NE. Rhodopsin splice site sequence changes in retinitis pigmentosa and their effect at the mRNA level. *Hum Mutat* 1998; Suppl 1S295-7. [PMID: 9452113].
36. Rosenfeld PJ, Hahn LB, Sandberg MA, Dryja TP, Berson EL. Low incidence of retinitis pigmentosa among heterozygous carriers of a specific rhodopsin splice site mutation. *Invest Ophthalmol Vis Sci* 1995; 36:2186-92. [PMID: 7558711].
37. Reig C, Alvarez AI, Tejada I, Molina M, Aróstegui E, Martín R, Antich J, Carballo M. New mutation in the 3'-acceptor splice site of intron 4 in the rhodopsin gene associated with autosomal dominant retinitis pigmentosa in a Basque family. *Hum Mutat* 1996; 8:93-4. [PMID: 8807346].

38. Rosenfeld PJ, Cowley GS, McGee TL, Sandberg MA, Berson EL, Dryja TP. A null mutation in the rhodopsin gene causes rod photoreceptor dysfunction and autosomal recessive retinitis pigmentosa. *Nat Genet* 1992; 1:209-13. [PMID: 1303237].
39. Sánchez B, Borrego S, Chaparro P, Rueda T, López F, Antiñolo G. A novel null mutation in the rhodopsin gene causing late onset autosomal dominant retinitis pigmentosa. *Hum Mutat* 1996; 7:180-[PMID: 8829640].
40. Kumaramanickavel G, Maw M, Denton MJ, John S, Srikumari CR, Orth U, Oehlmann R, Gal A. Missense rhodopsin mutation in a family with recessive RP. *Nat Genet* 1994; 8:10-1. [PMID: 7987385].
41. Kartasmita A, Fujiki K, Iskandar E, Sovani I, Fujimaki T, Murakami A. A novel nonsense mutation in rhodopsin gene in two Indonesian families with autosomal recessive retinitis pigmentosa. *Ophthalmic Genet* 2011; 32:57-63. [PMID: 21174529].
42. Towns KV, Kipioti A, Long V, McKibbin M, Maubaret C, Vaclavik V, Ehsani P, Springell K, Kamal M, Ramesar RS, Mackey DA, Moore AT, Mukhopadhyay R, Webster AR, Black GC, O'Sullivan J, Bhattacharya SS, Pierce EA, Beggs JD, Inglehearn CF. Prognosis for splicing factor PRPF8 retinitis pigmentosa, novel mutations and correlation between human and yeast phenotypes. *Hum Mutat* 2010; 31:E1361-76. [PMID: 20232351].
43. Martínez-Gimeno M, Gamundi MJ, Hernan I, Maseras M, Millá E, Ayuso C, García-Sandoval B, Beneyto M, Vilela C, Baiget M, Antiñolo G, Carballo M. Mutations in the pre-mRNA splicing-factor genes PRPF3, PRPF8, and PRPF31 in Spanish families with autosomal dominant retinitis pigmentosa. *Invest Ophthalmol Vis Sci* 2003; 44:2171-7. [PMID: 12714658].

Articles are provided courtesy of Emory University and the Zhongshan Ophthalmic Center, Sun Yat-sen University, P.R. China. The print version of this article was created on 18 August 2015. This reflects all typographical corrections and errata to the article through that date. Details of any changes may be found in the online version of the article.